Journal of Earth Science, *Vol. 28*, *No. 1*, *p. 103–112*, *February 2017* *ISSN 1674-487X*
Printed in China
DOI: 10.1007/s12583-017-0748-2

Geoelectrical Investigation of Groundwater Potentials of Northern Paiko, Niger State, North Central Nigeria

Usman D. Alhassan[1], **Daniel Nnaemeka Obiora***[2], **Francisca Nneka Okeke**[2]
1. *Department of Physics*, *Federal University of Technology*, *Minna*, *Nigeria*
2. *Department of Physics and Astronomy*, *University of Nigeria*, *Nsukka* 410001, *Nigeria*
Usman D. Alhassan: http://orcid-org/0000-0001-5376-5558; Daniel Nnaemeka Obiora: http://orcid-org/0000-0002-9893-0673

ABSTRACT: Vertical electrical sounding (VES) was carried out in northern part of Paiko, North Central Nigeria, using Abem terrameter model SAS 4000 to determine the subsurface layer parameters (resistivities, depths and thickness) employed in delineating the groundwater potential of the area. A total of six transverses with ten VES stations along each traverse, at intervals of 50 m were investigated. It has a maximum current electrode separation (AB/2) of 100 m. Three to four distinct geoelectric layers were observed, namely, the top layer, the weathered layer, the fractured/fresh layer, and the fresh basement layer. The observed frequencies in curve types include 21% of H, 4.2% of HA, 2.4% of K, 4.2% of A, 1.67% of KH and 3% of HK. Eight VES stations were delineated as ground water potentials of the area, with third and fourth layer resistivities ranging from 191 to 398 Ω·m. Depths range from 13.60 to 36.60 m and thickness varies from 9.23 to 30.51 m. A correlation of the borehole log with the VES lithology is in agreement. Viable boreholes for good portable water should be sited at VES stations J_8 and J_{10} having a fine aquifer at a depth of 36.60 and 17.80 m respectively with thickness of 30.51 and 15.07 m, respectively.

KEY WORDS: vertical electrical sounding, groundwater potential, northern Paiko, resistivity, aquifer, geoelectric layer, Abem terrameter.

0 INTRODUCTION

Paiko (the study area) is headquarter of Paikoro local government area in Niger State, North Central Nigeria. The population of Paiko is increasing rapidly as a result of new state University (Ibrahim Badamasi Babagida University, Lapai) locating around the area. As such, hand-dug wells and surface water is no longer sufficient to sustain the need of the growing population. However, hand-dug wells and surface water has their inherent problem of easy contamination from human and animal activities, hence, they are not reliable sources of potable water. Therefore, it is great need to locate areas that would be potentially viable for groundwater development. At the moment, there is only one known geophysical survey conducted in Paiko (Dangana, 2007). In Nigeria, as surface water becomes increasingly polluted, people turn to groundwater for alternative supplies (Dauda, 1993). Groundwater is an important water resource in both the urban and rural areas of Nigeria. The availability of quality water resources has always been the primary concern of every society in semi-arid and arid regions, even in areas of more abundant rainfall. The problem of obtaining adequate supply of quality water is generally becoming more acute due to ever increasing population and industrialization. As a result of this, surface water cannot be dependable throughout the year, hence, the need to look for other alternatives to supplement surface water. This makes the world depend on the largest available source of quality fresh water which lies underground, referred to, as groundwater. Groundwater is about 20% of the world's fresh water supply, which is about 0.61% of entire world's water, including the oceans and permanent ice.

Among several geophysical methods employed in groundwater exploration (electrical resistivity, gravity, seismic, magnetic, remote sensing and electromagnetic), the electrical resistivity method is the most effective for locating productive wells. It is an effective and a reliable tool in locating viable aquifers for continuous and regular water supply (Todd and Mays, 2005). It has the advantage of non-destructive effect on the environment, cost effective, rapid and quick survey time and less ambiguity interpretations of results when compared to other geophysical survey methods (Todd, 1980). The vertical electrical sounding (VES) technique provides information on the vertical variations in the resistivity of the ground with depth (Ariyo, 2005). It is used to solve a wide variety of groundwater problems, such as determination of depth, thickness and boundary of aquifers (Bello and Makinde, 2007; Asfahani, 2006), determination of zones with high yield potential in an aquifer (Akaolisa, 2006; Oseji et al., 2005) and determination of groundwater quality (Arshad et al., 2007). VES has been employed extensively in groundwater investigations in many basement complex terrains

*Corresponding author: daniel.obiora@unn.edu.ng

Manuscript received August 16, 2014.
Manuscript accepted March 18, 2015.

Alhassan, U. D., Obiora, D. N., Okeke, F. N., 2017. Geoelectrical Investigation of Groundwater Potentials of Northern Paiko, Niger State, North Central Nigeria. *Journal of Earth Science*, 28(1): 103–112. doi:10.1007/s12583-017-0748-2. http://en.earth-science.net

of Africa (Adeniji et al., 2013; Olayinka and Olorunfemi, 1992; Barongo and Palacky, 1991; Palacky, 1989).

Amadi et al. (2011) carried out a study of groundwater potential of Pompo Village in the neighborhood of Gidan Kwano campus of Federal University of Technology, Minna, using vertical electrical resistivity sounding. They carried out a total of 12 vertical electrical soundings (VES) across the area using the Schlumberger electrode array configuration. Their vertical electrical sounding curves revealed that the area is generally characterized by five geo-electric layers. The top soil layer is a highly resistive layer with thickness ranging from 0.3 to 1.6 m. The second geo-electric layer is a resistive dry layer with thickness ranging from 0.9 to 4.3 m. The weathered basement layer thickness varies from 0.9 to 9.1 m. The fractured basement ranges from 2.1 to 16.4 m in thickness, while the depth to basement varies between 4.9 and 25.3 m. They delineated two types of aquifers, which are the weathered basement and fractured basement aquifer and suggested that these aquifer units may have significant groundwater potential. Anudu et al. (2011) carried out geoelectric sounding for groundwater exploration in the crystalline basement terrain around Onipe and adjoining areas, southwestern Nigeria. Onipe and adjoining areas are underlain by Pre-Cambrian basement rocks and the dominant rock types are banded gneiss and quartzite. They conducted 16 geoelectric soundings (VES) using the Schlumberger array across the area. Their results showed three to four geoelectric layers, namely, the topsoil (84–1 165 Ω·m), weathered basement rock (22–436 Ω·m), fractured basement rock (156–2 973 Ω·m) and fresh basement rock (3 419–13 695 Ω·m). The weathered and fractured basement rocks constitute the aquifers or aquiferous zones in the area.

Arabi et al. (2011) carried out evaluation of aquifer potentials for irrigation practice in parts of the basement complex of North-Central Nigeria using vertical electrical sounding with the aim of using the results to delineate aquifer and assess its sustenance for adequate water supply for irrigation work in Fadama parts of some villages in Igabi local government area, Kaduna State, Nigeria. They acquired the data with symmetric Schlumberger configuration. Their interpreted results suggested four geoelectric layers. From their equivalent geologic/lithologic units, the weathered and the underlain fractured basement, which are characterized with relatively low resistivity values (14–217 Ω·m), were considered as the aquiferous layers of the study area. Ibrahim et al. (2012) used geoelectrical soundings to investigate groundwater potential of Orisunmibare Village in Ilorin south area of Kwara State, Nigeria. They conducted a total of nine VES in different parts of the study area with DDR1 resistivity meter equipped with an SAS 2000 booster by means of Schlumberger electrode array configuration. Their results revealed that the area is characterized by five classes of geoelectric layers. First, highly resistive topsoil layer has a thickness between 0.2–1.0 m. The second lateritic clay layer has thickness ranging of 3.3–15.0 m. The third layer is highly weathered basement with thickness of 6.0–30.7 m. The fourth fractured with weathered rock layer has thickness from 20.0–40.2 m, and fresh basement representing fifth layer has a thickness from 20 m and above. Their results indicated the occurrence of good aquifers in the form of the weathered and fractured basement. They also indicated that borehole drilling in the study area is achievable but to a depth of 45 m to allow large reservoir within the aquifers. Adeniji et al. (2013) investigated the groundwater potentials of Bwari basement area using solely geoelectric surveys with twenty vertical electrical soundings conducted along different transverses with maximum electrode spacing of 300 m. Their results revealed that the area is characterized with 3 to 6 geoelectric subsurface layers with variability in resistivities and thicknesses of the different layers. They observed that the weathered or weathered fractured layer constitute the water saturation zone or aquifereous units. They categorized areas where weathered layer thickness is greater than 25 m and of low clay content as indicated by the resistivity (>150 Ω·m) value to be areas of high groundwater potentials.

Resistivity is a principle that is governed sorely by pore fluid content or matrix mineral. If the matrix mineral is highly conductive (gold, clay, galena, etc.), the resistivity will be low. If pore fluid is water, resistivity will also be low. There is a clear absence of conductive minerals on the outcrops; therefore, low resistivity response can only be due to the presence of groundwater in the fractures.

1 GEOLOGY OF THE STUDY AREA

Paiko, the headquarters of Paikoro local government area of Niger State in the north central part of Nigeria, falls within the north central Nigerian basement complex. It is underlain by rocks of the Nigerian basement complex comprising magmatite-gneiss complex, younger metasediments, older and younger granites. It has an elevation of 304 m above sea level with population of about 736 133 as at 2006 census. It is bounded by latitudes 9º25′N and 9º27′N and longitudes 6º37′E and 6º39′E. Generally, the area mapped forms part of the Minna-granitic formation that consists of metasediment and metavolcanics. The metasediment include quartzites, gneisses and the metavolcanics are mainly granites. Among the main rock groups are granites which occur at the central and northern parts of the area, while on the south and east, cobbles of quartzite are found especially along the channels and valley. However, the other bodies like pegmatites and quartz veins also occur within the major rock types (Fig. 1a). The rocks are mainly biotite-granites with medium to coarse grained, light colored rocks with variations in biotite content. The mineral constituents are leucocratic to mesocratic. However, the biotite minerals are thread like and are arranged rough parallel streak, although some are disoriented in the groundmass. The feldspar minerals occur as fine to medium grained, though grains are cloudy as a result of alteration mostly along the twin planes, while the quartz minerals are constituents of the granitic rocks which show strong fracturing in the granitic rocks of the area (Ajibade, 1980). The Paiko area is underlain by four geologic sections, namely, laterite, quartz, sandy clay as the first layer, weathered basement as the second layer, fractured basement as the third layer and fresh basement as the forth layer. It is also observed that a number of rock types which suffered weathering, fracturing and decompositions are granites and quartzites (Dangana, 2007). The low resistivity zone within the bedrock suggests that it is associated with fractured zone (Asry et al.,

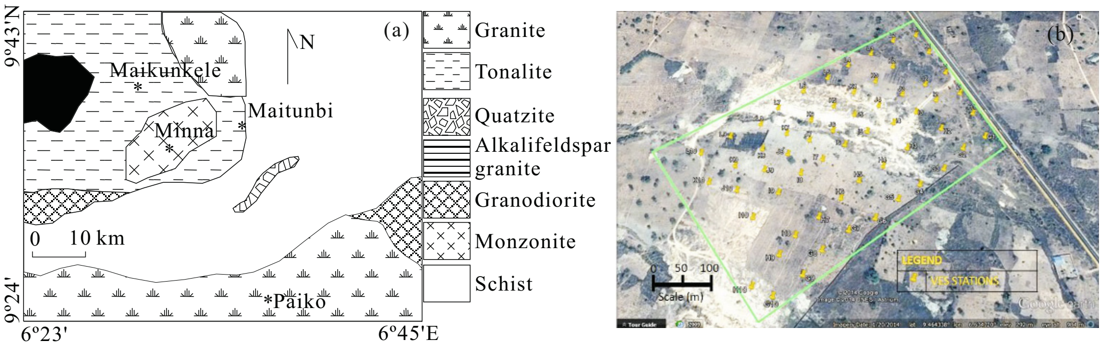

Figure 1. (a) Geological map of Minna (Alabi, 2011); (b) Google earth map of the study area.

2012). Groundwater occurrence in a Precambrian basement terrain is hosted within zones of weathering and fracturing which often are not continuous in vertical and lateral extent (Abubakar and Auwal, 2012; Jeff, 2006). The aquifers of the basement complex rocks are the regolith and the fractures in the fresh bed rock which are known to be interconnected at depth (Abubakar and Auwal, 2012).

The raining period runs from April to October with the highest amount of rainfall recorded in August while the average annual rainfall is between 1 200–1 300 mm. The mean annual temperature is between 22 to 25 ºC. The period between November and February are marked with the NE trend wind called the harmattan, which often causes very poor visibility during this period. There are three surface water available in the area but they are contaminated as a result of human and animals activities in the water.

2 METHODOLOGY

This research has utilized the electrical resistivity method in delineating the groundwater potential of the study area. Sixty vertical electrical soundings (Fig. 1b) were carried out using SAS 4000 model terrameter and its accessories. The conventional Schlumberger array pattern with half electrode spacing (AB/2) varying from 1 m to a maximum of 100 m was adopted. The electrical resistivity method uses a series of electrodes nailed into the ground about six inches deep along a selected straight profile. The distance between the electrodes depends on the desired depth of investigation and the target being imaged. The farther apart the electrodes are, the "deeper" the current goes into the earth, at the expense of resolution. The most commonly used configuration is the Schlumberger array which uses four electrodes at a time, two for passing current into the ground and two for measuring the potential difference. The resistivity measurements are usually made by injecting current into the ground through two current electrodes and measuring the resulting voltage difference at two potential electrodes. From the current (I) and voltage (V) values, an apparent resistivity (ρ_a) value is calculated using

$$\rho_a = K\frac{V}{I} \tag{1}$$

where K is the geometric factor which depends on the arrangement of the four electrodes and it is given as

$$K = \pi \cdot \left[\frac{\left(\frac{\text{AB}}{2}\right)^2 - \left(\frac{\text{MN}}{2}\right)^2}{\text{MN}} \right] \tag{2}$$

where AB/2 is half the distance between current electrodes A and B, MN/2 is half the distance between potential electrodes M and N.

$$R = \frac{V}{I} \tag{3}$$

where R is the resistance.

Hence Eq. (1) is written as

$$\rho_a = KR \tag{4}$$

If the ground is composed of an infinity-thick, homogeneous, and isotropic medium, then the resistivity calculated from Eq. 1 will be the true resistivity of that medium, otherwise the calculated resistivity is called an apparent resistivity (Zohdy et al., 1994). In general, for a heterogeneous medium, the apparent resistivity depends on the geometry, the spacing, and the orientation of the electrode array with respect to lateral inhomogeneities, and it also depends on the spatial distribution of materials with different electrical resistivities (Zohdy et al., 1994). An estimate of the distribution of the true resistivity of subsurface materials at various depths can be calculated from the apparent resistivities and the electrode spacing using many different interpretation methods. To make a symmetric Schlumberger sounding, the distance between the current electrodes, A and B, is increased at a succession of logarithmically-nearly-equal increments and the corresponding apparent resistivity is calculated from Eq. (4). The distance between the potential electrodes, M and N, is held fixed for a succession of expanding current electrode spacing. The expansion of the current electrode spacing is periodically stopped, and the distance between the potential electrodes is increased, and the apparent resistivity is recalculated at the expanded potential electrode spacing; then the expansion of the current electrode spacing is resumed. The main purpose of expanding the distance between potential electrodes is to increase the magnitude of the signal (potential difference) between the potential electrodes. To measure an approximation of the electric field (which is the gradient of the electric potential) at the center of the electrode configuration, the current electrode spacing, AB/2, must be greater than or equal to five times the potential electrode spacing, MN/2.

The potential and current electrode intervals ranged between 1–30 m (MN/2=0.5 to 15 m) and 2–200 m (AB/2=1 to 100 m), respectively. The coordinates of the locations were taken using the Global Positioning System (GPS). The processing of apparent resistivity values with IPI2WIN software constrained by drilled borehole lithologic information led to the determination of the model curves used in this work. Resistivity, depth and thickness values of different layers that the current penetrated were determined from the curves as shown in Tables 1 and 2.

The reflection coefficients (R_C) and fracture contrasts (F_C) of the fresh basement rock of the groundwater potential of the study area were calculated using (Adeniji et al., 2013; Loke, 1999; Olayinka, 1996; Bhattacharya and Patra, 1968)

$$R_C = \frac{\rho_n - \rho_{n-1}}{\rho_n + \rho_{n-1}} \tag{5}$$

$$F_C = \frac{\rho_n}{\rho_{n-1}} \tag{6}$$

where ρ_n is the layer resistivity of the nth layer and $\rho_{n\text{-}1}$ is the layer resistivity overlying the nth layer. The apparent resistivity values obtained from Eq. (4) were plotted against the half current electrode separation spacing using IPI2WIN software. From these plots, qualitative deductions such as resistivity of the layers, the depth of each layer, the thickness of each layer and curve types were made (Fig. 2).

3 RESULTS AND DISCUSSION

The summary of the interpreted electrical resistivity survey is presented in Tables 1 and 2. Table 1 consists of VES stations G_1 to I_{10} while Table 2 comprised of VES stations J_1 to L_{10}. The geoelectric section (Figs. 3a–3f) reveals that the area is characterized by 3 to 4 geoelectric subsurface layers. Six transverses with sixty VES stations were covered and their subsurface geo-electric sections are presented in Fig. 3. From Fig. 3, the geo-electric subsurface section ranged from 3 to 4 layers with 3-layer type occurring more and it is characterized by H curve type, while some are characterized by A and K curve types. The 3-layer geoelectric sections are generally made up of topsoil, weathered/fractured layer and fresh basement rock from top to the bottom with variable depths, thicknesses and resistivities. The 4-layer geoelectric sections are characterized by HA and HK curve types. The observed frequencies in curve types include 21% of H, 4.2% of HA, 2.4% of K, 4.2% of A, 1.67% of KH and 3% of HK. The 4-layer geoelectric section is made up of topsoil, weathered layer, fractured layer and fresh basement rock. Generally, the topsoil of the area is made up of loose sand, gravels, sandy clay, laterite and clay. Weathered and fractured layers constitute the aquiferous units where they have appreciable depths, thicknesses and low resistivities in the basement complex terrain. The groundwater potential indices (Table 3) were used to determine the groundwater potentials of the study area (Table 4). The reflection coefficient at fresh basement rock interface can provide some insights into the aquiferous nature of the basement rocks. Olayinka (1996) observed that areas of lower reflection coefficient value exhibits a fracture of the basement rock, and hence, has a higher water potential. In this work, VES points with reflection coefficient between 0.24 and 0.99 are considered aquifer potentials (Table 4). Eight VES stations were delineated as ground water potentials of the area (Table 4), having fractured layer resistivities ranging from 191 to 398 Ω·m.

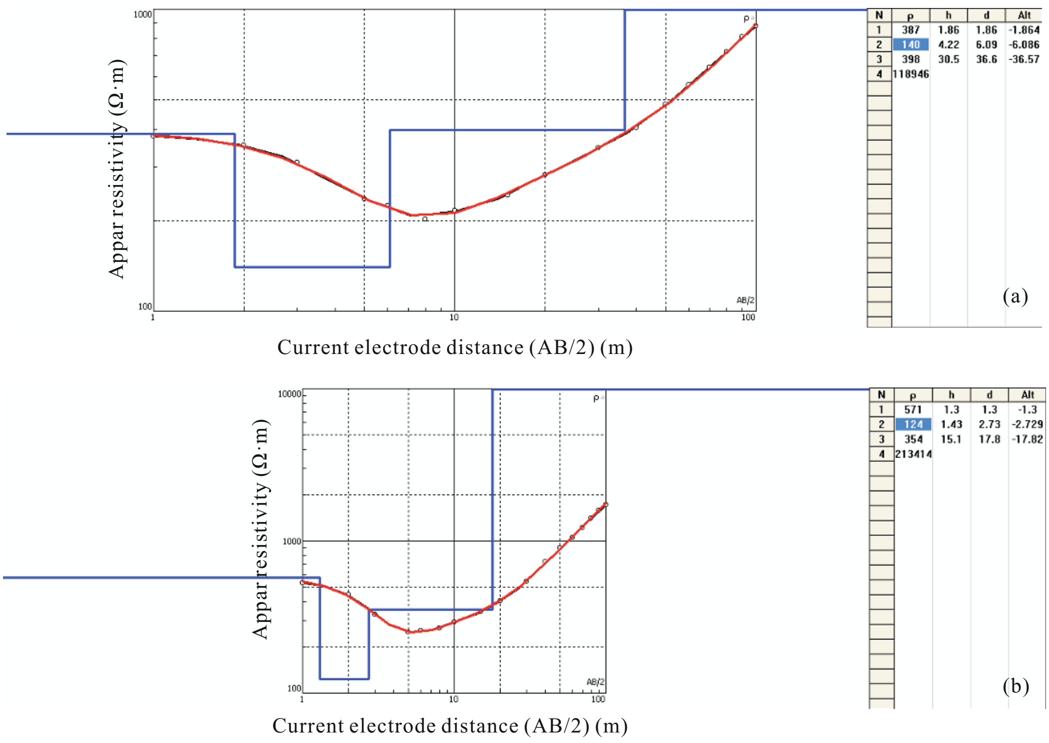

Figure 2. Diagrams showing (a) VES curve J_8; (b) VES curve J_{10}.

Table 1 Layer resistivities, depths, thicknesses and curve types of VES stations G_1 to J_{10}

VES station	Latitude (°)	Longitude (°)	No. of layer	Layer resistivity (Ω·m)				Layer depth (m)				Layer thickness (m)				Curve type
				ρ_1	ρ_2	ρ_3	ρ_4	d_1	d_2	d_3	d_4	h_1	h_2	h_3	h_4	
G_1	09.465 2	006.638 7	3	1 248	184	60 671		1.40	6.00	∞		1.40	4.60	∞		H
G_2	09.465 0	006.638 3	3	1 720	526	11 221		1.38	7.27	∞		1.38	5.89	∞		H
G_3	09.464 6	006.637 9	3	667	126	12 178		1.14	4.07	∞		1.15	2.92	∞		H
G_4	09.464 3	006.637 5	3	947	70.80	78 315		1.63	5.11	∞		1.63	3.47	∞		H
G_5	09.464 1	006.637 2	4	820	247	1 021	308 865	1.04	1.88	26.30	∞	1.04	0.85	24.40	∞	HA
G_6	09.463 7	006.636 8	3	380	8 244	1 522		2.87	4.91	∞		2.07	2.04	∞		K
G_7	09.463 6	006.636 4	3	1 120	132	4 920		2.07	3.93	∞		2.07	1.06	∞		H
G_8	09.463 3	006.636 0	3	419	968	15 552		3.91	23.30	∞		3.91	19.40	∞		A
G_9	09.462 9	006.635 7	3	229	11 184	1 303		2.11	6.87	∞		2.11	4.75	∞		K
G_{10}	09.462 6	006.635 3	3	117	351	13 298		1.18	9.07	∞		1.19	7.88	∞		A
H_1	09.465 6	006.638 5	4	1 490	152	750	117 922	1.18	3.21	25.40	∞	1.18	2.03	22.10	∞	HA
H_2	09.465 3	006.637 9	3	415	124	3 204		1.69	3.93	∞		1.69	2.24	∞		H
H_3	09.465 0	006.637 3	3	308	130	13 859		1.42	3.28	∞		1.42	1.86	∞		H
H_4	09.464 6	006.636 9	3	1 114	136	41 263		1.93	7.16	∞		1.93	5.23	∞		H
H_5	09.464 4	006.636 5	3	39.90	60 825	5 239		3.07	75.10	∞		3.07	72.00	∞		K
H_6	09.464 1	006.636 2	3	1 070	80 368	224		1.38	4.81	∞		1.38	3.43	∞		K
H_7	09.463 8	006.635 9	3	243	941	92 291		1.85	26.10	∞		1.05	24.30	∞		A
H_8	09.463 5	006.635 6	3	457	700	215 028		1.45	12.40	∞		1.45	10.90	∞		A
H_9	09.462 7	006.635 0	3	550	28	4 233		1.12	3.30	∞		1.12	2.17	∞		H
H_{10}	09.462 7	006.635 0	4	191	106	263	278 439	1.43	3.03	17.60	∞	1.43	1.60	14.60	∞	HA
I_1	09.466 0	006.638 3	3	595	46.40	194 453		1.37	3.34	∞		1.37	1.96	∞		H
I_2	09.465 9	006.637 9	3	761	110	3 542		1.25	4.10	∞		1.25	2.86	∞		H
I_3	09.465 7	006.637 5	3	536	153	7 580		1.52	4.75	∞		1.52	3.23	∞		H
I_4	09.465 5	006.637 1	3	527	32	103 681		1.16	5.47	∞		1.16	4.31	∞		H
I_5	09.465 3	006.636 7	3	180	27.70	55 673		1.22	5.23	∞		1.22	4.02	∞		H
I_6	09.465 1	006.636 3	3	1 606	154	1 796		1.12	3.72	∞		1.12	2.60	∞		H
I_7	09.464 8	006.635 9	3	764	34.10	2 027		1.06	2.18	∞		1.06	1.12	∞		H
I_8	09.464 5	006.635 6	3	3 082	131	43 827		2.15	8.22	∞		2.15	6.06	∞		H
I_9	09.464 2	006.635 2	3	474	27	38 527		1.61	3.97	∞		1.61	2.36	∞		H
I_{10}	09.463 8	006.634 9	3	1 463	10.90	19 302		1.11	2.78	∞		1.11	1.67	∞		H

VES. Vertical electrical sounding; ρ. layer resistivity; *d*. layer depth; *h*. layer thickness.

Table 2 Layer resistivities, depths, thicknesses and curve types of VES stations J_1 to L_{10}

VES station	Latitude (°)	Longitude (°)	No. of layer	Layer resistivity (Ω·m)				Layer depth (m)				Layer thickness (m)				Curve type
				ρ_1	ρ_2	ρ_3	ρ_4	d_1	d_2	d_3	d_4	h_1	h_2	h_3	h_4	
J_1	09.466 55	006.638 17	3	841	223	2 867		1.36	3.61	∞		1.36	2.25	∞		H
J_2	09.466 3	006.637 78	4	439	85.20	236 672	696	1.35	3.53	8.57	∞	1.35	2.18	5.04	∞	HK
J_3	09.466 10	006.637 36	3	1 423	978	9 225		8.53	15.70	∞		8.53	7.20	∞		H
J_4	09.465 87	006.636 93	4	985	189	94 441	288	1.05	3.27	11.20	∞	1.05	2.22	7.93	∞	HK
J_5	09.465 69	006.636 50	3	83.80	29.40	131 987		1.86	5.86	∞		1.86	3.99	∞		H
J_6	09.465 38	006.636 13	2	62.20	1 623			1.56	∞			1.56	∞			A
J_7	09.465 20	006.635 73	3	982	199	2 950		0.95	3.54	∞		0.95	2.59	∞		H
J_8	09.464 94	006.635 38	4	387	140	398	118 946	1.86	6.09	36.60	∞	1.86	4.22	30.50	∞	HA
J_9	09.464 65	006.635 01	3	620	11.20	58 241		1.00	3.00	∞		1.00	2.00	∞		H
J_{10}	09.464 29	006.634 60	4	571	124	354	213 414	1.30	2.73	17.80	∞	1.30	1.43	15.10	∞	HA
K_1	09.467 04	006.637 90	4	554	4 846	296	196 873	3.57	7.19	16.40	∞	3.57	3.61	9.22	∞	KH
K_2	09.466 72	006.637 21	3	636	978	5 752		4.06	26.20	∞		4.06	22.10	∞		A
K_3	09.466 40	006.636 88	3	517	78	5 437		1.17	3.22	∞		1.17	2.05	∞		H
K_4	09.466 17	006.636 49	3	178	111	6 005		1.42	4.47	∞		1.42	3.05	∞		H
K_5	09.465 88	006.636 13	4	469	117	191	134 745	1.07	3.00	15.70	∞	1.07	1.93	12.70	∞	HA
K_6	09.465 60	006.635 74	3	198	331	95 088		1.30	15.20	∞		1.30	13.90	∞		A
K_7	09.465 33	006.635 33	4	776	61.30	1 478	59 411	1.21	2.76	40.30	∞	1.21	1.54	37.50	∞	HA
K_8	09.465 04	006.634 94	3	712	61.20	108 026		1.06	7.45	∞		1.06	6.39	∞		H
K_9	09.464 73	006.634 51	3	786	114	29 362		2.02	16.10	∞		2.02	14.10	∞		H
K_{10}	09.464 43	006.634 12	3	433	113	1 038		2.02	3.62	∞		2.02	1.60	∞		H
L_1	09.467 46	006.637 68	4	300	196	27 962	79.90	2.69	7.93	15.30	∞	2.69	5.23	7.41	∞	HK
L_2	09.467 34	006.637 24	4	620	154	38 600	130	1.18	3.24	8.02	∞	1.18	2.06	4.78	∞	HK
L_3	09.467 03	006.636 81	4	625	132	113 317	303	1.28	3.03	6.78	∞	1.28	1.75	3.75	∞	HK
L_4	09.466 77	006.636 38	3	1 052	232	172 184		1.24	12.70	∞		1.24	11.40	∞		H
L_5	09.466 50	006.636 00	3	656	289	4 230		1.49	13.60	∞		1.49	12.10	∞		H
L_6	09.466 21	006.635 57	3	85	15.20	78 682		1.13	5.26	∞		1.13	4.13	∞		H
L_7	09.465 85	006.635 14	3	584	156	2 853		1.18	3.73	∞		1.18	2.55	∞		H
L_8	09.465 52	006.634 86	3	1 003	59.80	31 877		2.54	7.28	∞		2.54	4.75	∞		H
L_9	09.465 29	006.634 36	3	546	43.20	107 599		1.42	7.54	∞		1.42	6.12	∞		H
L_{10}	09.464 97	006.633 90	3	420	170	110 943		2.31	14.40	∞		2.31	12.10	∞		H

VES. Vertical electrical sounding; *ρ*. layer resistivity; *d*. layer depth; *h*. layer thickness.

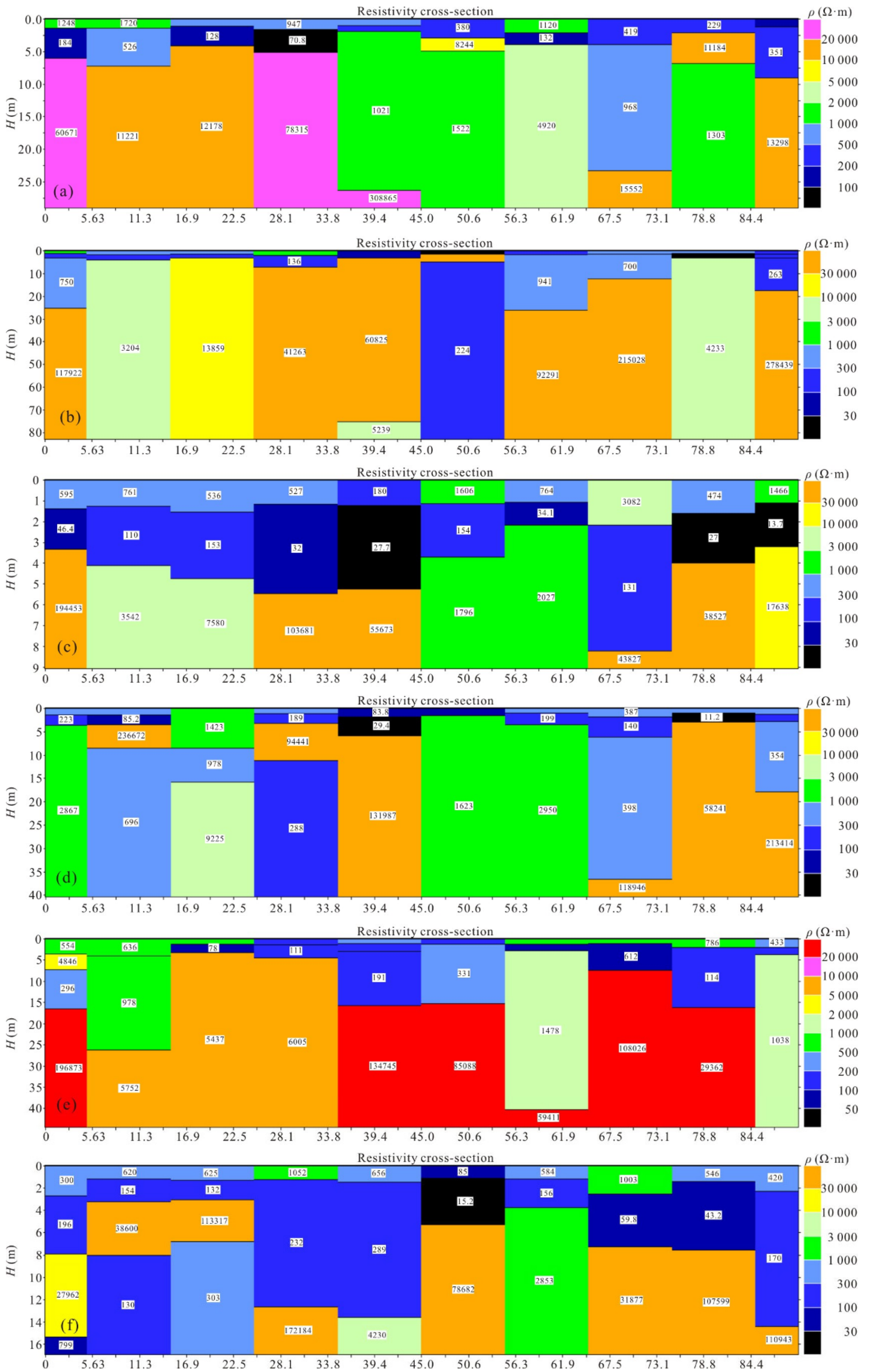

Figure 3. (a) Geoelectric section for tranverse G; (b) geoelectric section for tranverse H; (c) geoelectric section for tranverse I; (d) geoelectric section for tranverse J; (e) geoelectric section for tranverse K; (f) geoelectric section for tranverse L.

Table 3 Groundwater potential indices

VES stations	Weathered/fractured resistivity (Ω·m)	Weathered/fractured thickness (m)	Overburden depth (m)	Reflection coefficient R_C	Fracture contrast F_C
H_{10}	263	14.57	17.60	0.425 474	2.481 132
J_8	398	30.51	36.60	0.479 554	2.842 857
J_{10}	354	15.07	17.80	0.481 172	2.854 839
K_1	296	9.23	16.40	0.884 87	0.061 081
K_5	191	12.70	15.70	0.240 26	1.632 479
K_6	331	13.90	15.20	0.993 062	287.274 9
L_5	289	12.11	13.60	0.872 096	14.636 68
L_{10}	170	12.09	14.40	0.996 94	652.605 9

Table 4 Aquifer potentials of the area

VES stations	Latitude (°)	Longitude (°)	Layer number	Layer resistivity (Ω·m)	Layer depth (m)	Layer thickness (m)	Curve type
H_{10}	09.46270	006.635 00	3	263	17.60	14.57	HA
J_8	09.464 94	006.635 38	3	398	36.60	30.51	HA
J_{10}	09.464 29	006.634 60	3	354	17.80	15.07	HA
K_1	09.467 04	006.637 90	3	296	16.40	9.23	KH
K_5	09.465 88	006.636 13	3	191	15.70	12.70	HA
K_6	09.465 60	006.635 74	2	331	15.20	13.90	A
L_5	09.466 50	006.636 00	2	289	13.60	12.11	H
L_{10}	09.464 97	006.633 90	2	170	14.40	12.09	H

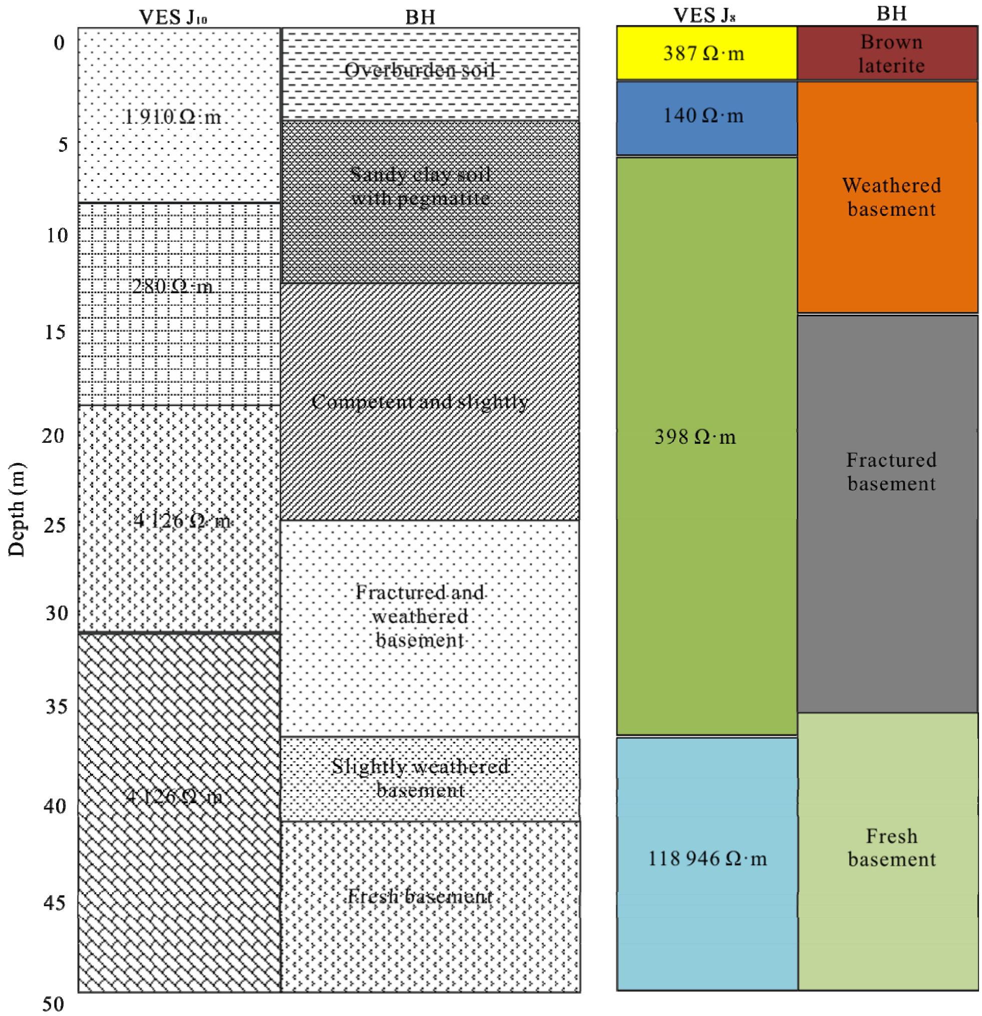

Figure 4. Correlation of VES lithology with nearby borehole logs.

The depths of these weathered/fractured layers are found to be from 13.60 to 36.60 m and thickness varies from 9.23 to 30.51 m as shown in Table 4. In a basement complex terrain, areas with overburden thickness of 15 m and above, and fractured layer resistivity of less than 400 Ω·m are good for groundwater development. The highest groundwater yield is often obtained from a fractured aquifer or a subsurface sequence that has a combination of a significantly thick and sandy weathered layer and fractured aquifer (Olorunfemi, 2009). A correlation of the nearby borehole log with the VES lithological formation is in agreement (Fig. 4). Results of the nearby boreholes pumping test are presented in Table 5. VES stations J_8 and J_{10} are observed to be the best aquifer potentials of the area, having a fine aquifer at a depth of 36.60 and 17.80 m respectively with fractured layer thickness of 30.51 and 15.07 m respectively as shown in Table 3.

In investigating the continuous variation of resistivity with depth, isoresistivity map using Golden Surfer 11.0 version was obtained for the layers. It shows the color range corresponding to resistivity values of the earth materials. The isoresistivity map of the first layer reveals that blue represent gravels, sky blue represents sand, green corresponds to laterite and yellow represents alluvial deposits (Fig. 5a). The isoresistivity map of the second layer shows that blue color corresponds to clay; sky blue represents groundwater and green corresponds to alluvial deposits (Fig. 5b). Third layer isoresistivity maps reveal that blue represent granite, sky blue represents gneiss, green corresponds to igneous rock, yellow represents gabbros rock and red corresponds to ultramafic rock (Fig. 5c).

Table 5 Nearby boreholes pumping test (Niger State Rural Water Supply and Sanitation)

Parameters	Borehole 1	Borehole 2	Borehole 3	Borehole 4	Borehole 5
Borehole depth	54 m	50 m	45 m	48 m	50 m
Static water level	5.96 m	4.78 m	4.11 m	3.63 m	8.09 m
Pump type and capacity	Franklin 1 hp	Same	Same	Same	Same
Top of casing above ground level	0.2 m	0.2 m	0.29 m	0.15 m	0.25 m
Pump setting	20 m	40 m	20 m	20 m	34.5 m
Borehole yield	75 L/min	16 L/min	56 L/min	70 L/min	60 L/min
Water level	37.45 m	37.11 m	7.52 m	18.69 m	21.24 m
Drawn down	31.49 m	32.33 m	3.41 m	15.06 m	13.15 m
Recovery drawn down	31.49 m	32.33 m	3.41 m	15.06 m	13.15 m

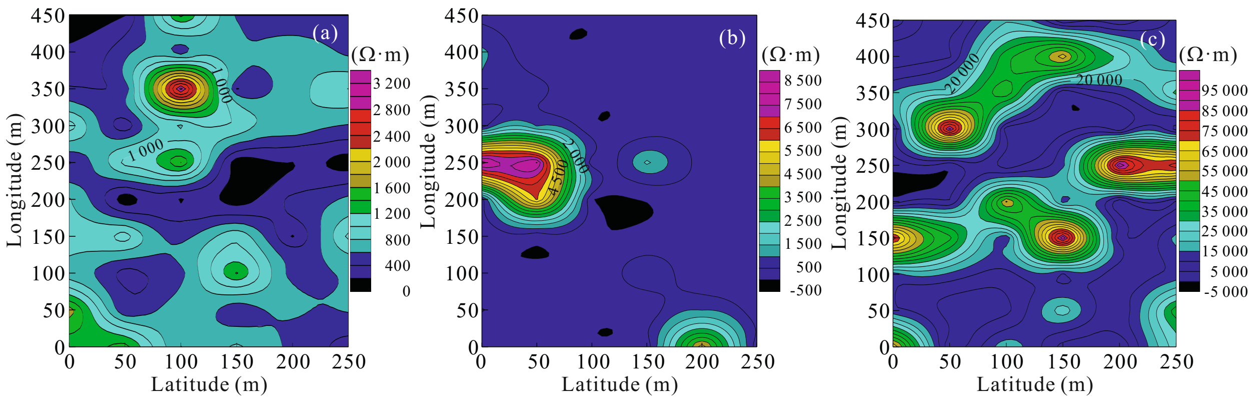

Figure 5. (a) Isoresistivity map for layer one, (b) layer two, and (c) layer three.

4 CONCLUSION

Groundwater usually occurs in discontinuous aquifers in basement complex area. Defining the potentials of the aquifers is normally a tedious exercise because of the intricate properties of the basement rocks (Adeniji et al., 2013). Therefore the use of various electrical resistivity parameters (resistivities of the fractured layer, depth of the layer and thickness of the layer) was employed in classifying the groundwater potentials of the study area. Results of this work reveal that the area is characterized by 3 to 4 geoelectric/geologic subsurface layers. Eight VES stations were delineated as ground water potentials of the area, having fractured layer resistivities ranging from 191 to 398 Ω·m. The depths of these weathered/fractured layers are found to be from 13.60 to 36.60 m and thickness varies from 9.23 to 30.51 m. VES stations J_8 and J_{10} are observed to be the best aquifer potentials of the area, having a fine aquifer at a depth of 36.60 and 17.80 m respectively with fractured layer thickness of 30.51 and 15.07 m respectively. From the isoresistivity maps produced, the earth materials of the area were identified which comprises of gravels, sand, laterite, alluvial deposits, clay, granite, gneiss, igneous, gabbros and ultramafic rocks. Groundwater developments can be concentrated in the areas of possible groundwater potentials as indicated in Table 3. Government and individuals who wish to site boreholes in Paiko area are encouraged to make use of the results of this study to reduce the problem of supplying quality water to the area.

More research work in this area would contribute to solving the water problem completely.

ACKNOWLEDGMENTS

The authors are grateful to Mr. Victor Omonona, and the editors and the reviewers for their useful comments. The final publication is available at Springer via http://dx.doi.org/10.1007/s12583-017-0748-2.

REFERENCES CITED

Abubakar, Y. I., Auwal, L. Y., 2012. Geoelectrical Investigation of Groundwater Potential of Dawakin Tofa Local Government Area of Kano State, Nigeria. *American International Journal of Contemporary Research*, 2(9): 1–10

Adeniji, A. E., Obiora, D. N., Omonona, O. V., et al., 2013. Geoelectrical Evaluation of Groundwater Potentials of Bwari Basement Area, Central Nigeria. *International Journal of Physical Sciences*, 8(25): 1350–1361

Ajibade, A. C., 1980. The Geology of the Country around Zungeru, Northwestern State of Nigeria: [Dissertation]. University of Ibadan, Ibadan. 59–70

Akaolisa, C., 2006. Aquifer Transmissivity and Basement Structure Determination Using Resistivity Sounding at Jos, Plateau State, Nigeria. *Environ. Monitor. Assess.*, 114: 27–34

Alabi, A. A., 2011. Geology and Environmental Impact Assesment and Benefit of Granitic Rocks of Minna Area, Northwestern Nigeria. *Ethiopian Journal of Environmental Studies and Management*, 4: 39–45

Amadi, A. N., Nwawulu, C. I., Unuevho, N. O., et al., 2011. Evaluation of the Groundwater Potential in Pompo Village, Gidan Kwano, Minna, Using Vertical Electrical Resistivity Sounding. *British Journal of Applied Science & Technology*, 1(3): 53–66

Anudu, G. K., Onuba, L. N., Ufondu, L. S., 2011. Geoelectric Sounding for Groundwater Exploration in the Crystalline Basement Terrain around Onipe and Adjoining Areas, Southwestern Nigeria. *Journal of Applied Technology in Environmental Sanitation*, 1(4): 343–354

Arabi, A. S., Raimi, J., Ibrahim, A. A., et al., 2011. Evaluation of Aquifer Potentials for Irrigation Practice in Parts of the Basement Complex of North Central Nigeria. *British Journal of Applied Science & Technology*, 1(4): 181–189

Ariyo, S. O., 2005. Geoelectrical Characterisation of Aquifers and Geochemical Study of Groundwater in the Basement Complex/Sedimentary Transition Zone around Isharsa, Southwest Nigeria: [Dissertation]. University of Ibadan, Nigeria. 34–55

Arshad, M., Cheema, J. M., Ahmed, S., 2007. Determination of Lithology and Groundwater Quality Using Electrical Resistivity Survey. *Int. J. Agric. Biol.*, 9: 143–146

Asfahani, J., 2006. Geoelectrical Investigation for Characterizing the Hydrogeological Conditions in Semi-Arid Region in Khanasser Valley, Syria. *J. Arid Environ.*, 68: 31–52

Asry, Z., AbdulRahim, S., Wanzuhari, Y., et al., 2012. Geoelectrical Resistivity Imaging and Refraction Seismic Investigations at Sg. Udang, Melaka. *American Journal of Engineering and Applied Sciences*, 5(1): 93–97

Barongo, J. O., Palacky, G. J., 1991. Investigations of Electrical Properties of Weathered Layers in the Yala Area, Western Kenya, Using Resistivity Soundings. *Geophys.*, 56(O.I): 133–138

Bello, A. A., Makinde, V., 2007. Delineation of the Aquifer in the South-Western Part of the Nupe Basin, Kwara State, Nigeria. *J. Am. Sci.*, 3: 36–44

Bhattacharya, P. K., Patra, H. P., 1968. Direct Current Geoelectric Sounding Methods in Geophysics. Elsevier, Netherland. 135

Dangana, L. M., 2007. Geoelectric Survey for Subsurface Water in Paiko Town, Niger State, Nigeria: [Dissertation]. University of Abuja, Nigeria. 50–60

Dauda, A. M., 1993. A Comprehensive Approach in Water Resource Management for the 21st Century. Environment Bullets, vol. 12, Nigeria

Ibrahim, K. O., Olasehinde, P. I., Akinrinmade, A. O., et al., 2012. Geoelectrical Soundings to Investigate Groundwater Potential of Orisunmibare Village in Ilorin South Area of Kwara State, Nigeria. *Journal of Environment*, 1(1): 21–25

Jeff, D., 2006. Forum for Groundwater. (2012-12-30) [2014-10-30]. http://www.waternet.co.za/groundwater/(3)

Loke, M. H., 1999. Electrical Imaging Survey for Environmental and Engineering Studies—A Practical Guide to 2-D and 3-D Surveys: Pre Conference Workshop Notes W2. The Theory and Practice of Electrical Imaging, EEGS. European Section 5th Meeting, Budapest, Hungary Niger State Water and Sanitation Board, Minna

Olayinka, A. I., 1996. Non Uniqueness in the Interpretation of Bedrock Resistivity from Sounding Curves and Its Hydrological Implications. *Water Resources Journal NAH*, 7(1/2): 55–60

Olayinka, A. I., Olorunfemi, M. O., 1992. Determination of Geoelectrical Characteristic in Okene Area and Implication for Boreholes Setting. *J. Min. Geol.*, 28: 403–412

Olorunfemi, M. O., 2009. Water Resources Groundwater Exploration Borehole Site Selection and Optimum Drill Depth in Basement Complex Terrain. *Journal of Nigerian Association of Hydrogeologists*, 1: 1–20

Oseji, J. O., Atakpo, E. A., Okolie, E. C., 2005. Geoelectric Investigation of the Aquifer Characteristics and Groundwater Potential in Kwale, Delta State, Nigeria. *J. Applied Sci. Environ. Mgt.*, 9: 157–160

Palacky, G. J., 1989. Resistivity characteristics of Geologic Targets. *Electromagnetic Methods in Applied Geophysics*, 1(3): 53–129

Todd, K. D., Mays, L. W., 2005. Groundwater Hydrology, 3rd Edition. John Wiley and Sons, New York. 652

Todd, K. D., 1980. Groundwater Hydrology, 2nd Edition. John Wiley and Sons, New York. 602

Zohdy, A. A. R., Bisdorf, R. J., Gates, J. S., 1994. A Direct Current Resistivity Survey of the Beaver Dam Wash Drainage in Southwest Utah, Southeast Nevada, and Northwest Arizona. *U.S. Geological Survey Open-File Report*, 87: 94–676